

# SBUV observations of polar mesospheric clouds compared with MLS temperature and water vapor measurements

Eric P. Shettle,<sup>1,2</sup> Gerald E. Nedoluha,<sup>1</sup> Matthew T. DeLand,<sup>3</sup> Gary E. Thomas,<sup>4</sup> and John J. Olivero<sup>5</sup>

Received 28 May 2010; revised 21 July 2010; accepted 5 August 2010; published 25 September 2010.

[1] Earlier studies have shown that Polar Mesospheric Clouds (PMC) occur more frequently in the northern hemisphere (NH) than the SH, consistent with colder NH temperatures. Coincident PMC observations with the Solar Backscatter Ultraviolet instruments on the NOAA-16 and NOAA-18 satellite and temperature and water vapor measurements with the Microwave Limb Sounder on the Aura satellite support this result. These coincident measurements also show that, for similar temperatures and water vapor mixing ratios, PMCs occur more frequently and are brighter in the NH than the SH. Possible reasons for these hemispheric differences are discussed. **Citation:** Shettle, E. P., G. E. Nedoluha, M. T. DeLand, G. E. Thomas, and J. J. Olivero (2010), SBUV observations of polar mesospheric clouds compared with MLS temperature and water vapor measurements, *Geophys. Res. Lett.*, 37, L18810, doi:10.1029/2010GL044132.

## 1. Introduction

[2] Polar Mesospheric Clouds (PMC) form in the upper mesosphere (~80 to 86 km) poleward of 50° latitude during the summers in each hemisphere. These clouds are formed of water ice particles [Hervig *et al.*, 2001; Eremenko *et al.*, 2005], and so will form only where the temperatures are cold enough for water vapor to be saturated relative to ice. It has been observed that more PMCs occur in the Northern Hemisphere (NH) than the SH, consistent with the colder NH temperatures [e.g., Hervig and Siskind, 2006; Wrotny and Russell, 2006]. This paper supports that finding, by using observations of PMCs made by the Solar Backscatter Ultraviolet (SBUV/2) instrument on the NOAA-16 and NOAA-18 polar orbiting satellites together with coincident measurements of atmospheric temperature and water vapor made by the Microwave Limb Sounder (MLS) instrument on Aura. These satellites have nearly the same equator crossing time (~1345) although with slightly different orbital altitudes and periods. This means about every 30 orbits Aura will catch up with and pass underneath the NOAA satellites, providing a series of coincident observations from the two satellite platforms. We obtain several thousand coincidences poleward of 50° latitude during each PMC season (30 days prior to

Summer solstice to 70 days after). We analyze five seasons of coincidences in the SH and four seasons in the NH, starting with the SH summer 2004–05. Sections 2 and 3 describe the SBUV and MLS measurements respectively, and the results are presented in Section 4, and discussed in Section 5.

## 2. SBUV Measurements

[3] The SBUV and SBUV/2 instruments were developed to measure stratospheric ozone [Heath *et al.*, 1975]. They make nadir viewing measurements of backscattered radiation at 12 wavelengths from 252.0 to 339.8 nm to determine the vertical ozone profile. Thomas *et al.* [1991] showed that these data could be used to measure PMC occurrence frequency and brightness. Their approach was used by DeLand *et al.* [2003] to look at long-term variations in PMC properties. The detection algorithm was improved by DeLand *et al.* [2007] to produce a version 3 PMC product which is used in the present study. The brightness of the detected PMCs in nadir-viewing geometry is typically only 4% to 10% of the background albedo. This means that SBUV only detects the brightest PMCs above normal background variations caused by ozone variability.

## 3. Microwave Limb Sounder Measurements

[4] The MLS instrument on the Aura spacecraft [Waters *et al.*, 2006] was designed to measure temperature, ClO, O<sub>3</sub>, H<sub>2</sub>O, plus a number of other atmospheric species. The MLS microwave radiometer scans the atmospheric limb looking forward along the orbit, so the actual measurement point is about 3000 km in front of the Aura satellite. The Aura satellite was launched on 15 July 2004 with the MLS instrument beginning operation mid-August 2004. For the present study our interest is in the temperature and water vapor products. The temperature is derived from measurements of the 118 and 234 GHz oxygen lines. In the upper mesosphere it is measured with a precision of ~3 K, and has a vertical resolution of about 14 km [Schwartz *et al.*, 2008]. The horizontal resolution is 200 km along the line-of-sight (LOS) by 6 km cross-track. During the polar summers, MLS shows a warm bias in the upper mesosphere relative to the Sounding of the Atmosphere using Broadband Radiometry (SABER) instrument [see Schwartz *et al.*, 2008, Figure 22]. (Only the MLS comparisons with SABER are available at high latitudes. The comparisons for other latitudes and seasons and with other instruments generally differ by less than 5 K.) Comparisons between MLS and SABER near the mesopause are complicated by the anomalously low mesopause in v1.06 SABER data. The water vapor is derived from the 183.3 GHz line using the 190 GHz radiometer. In the upper meso-

<sup>1</sup>Naval Research Laboratory, Washington, D. C., USA.

<sup>2</sup>Retired

<sup>3</sup>Science Systems and Applications, Inc., Lanham, Maryland, USA.

<sup>4</sup>Laboratory for Atmospheric and Space Physics, University of Colorado, Boulder, Colorado, USA.

<sup>5</sup>Department of Physical Sciences, Embry-Riddle Aeronautical University, Daytona Beach, Florida, USA.

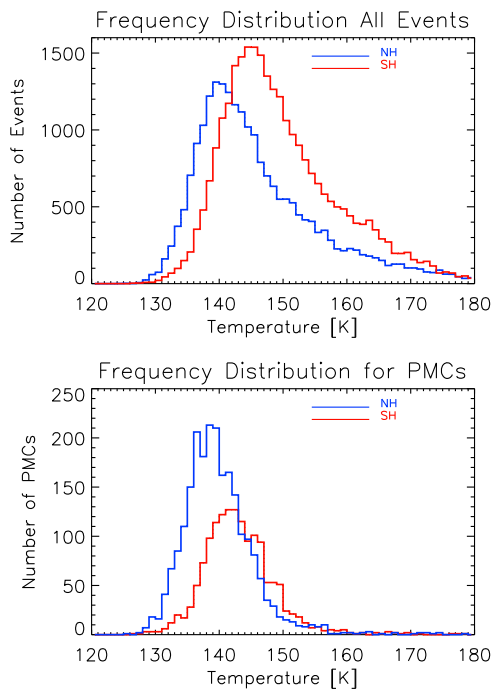


**Figure 1.** (top) Number of SBUV measurements in each 1 K temperature interval for NH (blue) and SH (red) summed over all available seasons. (bottom) Number of PMC detections in each hemisphere summed over all seasons.

sphere the water vapor has a vertical resolution of  $\sim 12$ – $16$  km [Lambert *et al.*, 2007], a horizontal resolution of 300 to 400 km by 6 km and has an uncertainty of about 1.2 ppmv ( $\sim 34\%$ ).

#### 4. Analysis

[5] Both NOAA-18 and Aura are in sun-synchronous orbits with an equator crossing-time near 1345 h. This means even with different altitudes (854 km vs. 705 km) and periods (102 min vs. 99 min), there will be frequent coincidences. Approximately every 30 orbits Aura will catch up with and pass directly underneath NOAA-18. We define a coincidence by requiring the location of the MLS measurement to be inside the SBUV/2 170 km  $\times$  170 km nadir field of view, within 15 minutes of the SBUV/2 measurement. This is a short enough time interval to assume that there has been no significant change in the cloud or atmospheric properties when averaged over the instrumental fields of view and cloud motions will be small compared to the SBUV/2 field of view. NOAA-18 was launched in May 2005, with the first PMC measurements taken in June 2005. For the 2004–05 Southern Hemisphere (SH) PMC season, the NOAA-16 satellite (which carries an SBUV/2 instrument) also provided frequent coincidences with MLS measurements. We therefore have useful coincidence data available for five SH PMC seasons (2004–05 through 2008–09) and four NH seasons (2005 through 2008), where we define the PMC season as extending from 30 days before Summer Solstice to 70 days afterwards.

[6] The SBUV/2 measurements of PMCs provide no information on their altitude, so for simplicity we interpolate the MLS measurements at 0.01 hPa and 0.0046 hPa to a pressure of 0.006 hPa, which corresponds to a typical PMC

altitude of about 83 km. The altitude of the 0.006 hPa pressure level reflects the  $\sim 1$  km increase in PMC altitude from  $50^\circ$  to  $80^\circ$  latitude and about half of the  $\sim 1$  km greater altitude of PMCs in the SH relative to the NH, as shown by lidar and other measurements [Lübken *et al.*, 2008]. Rather than directly using the MLS water vapor product, we calculate the saturation ratio (the ratio of the interpolated water vapor pressure to the saturation vapor pressure with respect to ice), using the parameterization of Murphy and Koop [2005].

[7] Combining data from all seasons, we find more than 20,000 coincidence events over four NH seasons with 2,295 PMCs detected, and more than 26,000 events over five SH seasons with 1,496 PMCs detected. Figure 1 shows how the number of events varied with temperature. The temperatures at 0.006 hPa were generally lower in the NH than in the SH, with more than twice as many measurements below 140 K.

[8] The frequency of occurrence (FO) of the PMCs in these data as a function of temperature is shown in Figure 2 (top), and as a function of saturation ratio ( $S$ ) in Figure 2 (bottom). As would be expected, the FO increases with decreasing temperatures and with increasing  $S$ . If the ice phase water was in equilibrium with the water vapor at a given temperature we would expect that the FO would simply depend on the temperature or saturation ratio independent of the hemisphere. However, there is also the unexpected result that for a given temperature or a given  $S$ , there is a higher FO of PMC in the NH than in the SH. Possible explanations for this are discussed in the following section. It should be noted that in Figure 2 (and Figures 3 and 4) a few points have been excluded where the uncertainties due to limited sampling are too large to make meaningful comparisons.

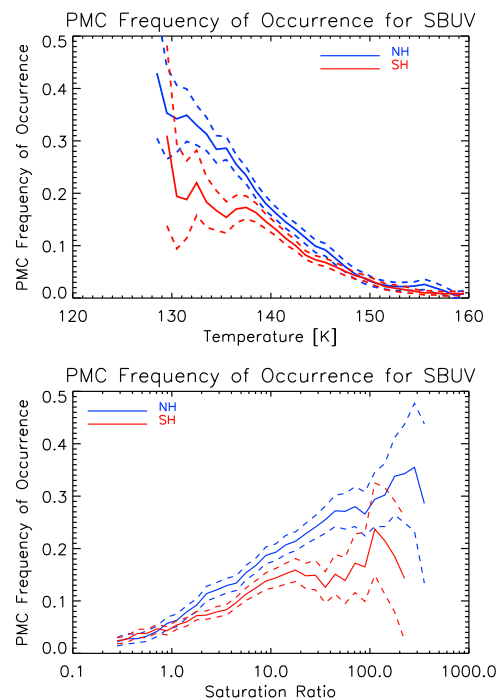


**Figure 2.** (top) The PMC frequency of occurrence as a function of temperature in each hemisphere. (bottom) The PMC frequency of occurrence as a function of saturation ratio in each hemisphere. The dashed lines in each panel indicate the 2 standard deviation confidence limits.

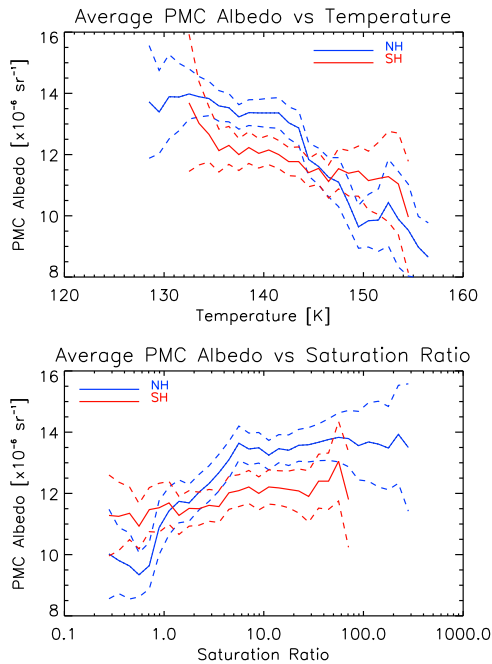


**Figure 3.** Average PMC albedo (top) as a function of Temperature and (bottom) as a function of Saturation Ratio.

[9] Only for the largest  $S$  values does the FO of PMCs approach 0.5. This is due in part to the nature of the SBUV PMC detection algorithm, which detects PMCs as the brightest events in a distribution of measurements. The SBUV field of view also averages a large horizontal region that may be only partially filled by a PMC, and may not increase the albedo by enough to be detected. This means, even if most of the coincidence events include PMCs within the SBUV field of view, only the brightest ones will be identified as such.

[10] The non-negligible FO of PMCs when the  $S$  value is less than 1.0 (ice crystals are unstable in unsaturated air) has several possible explanations: (i) The PMCs are typically 2 to 3 km thick compared with the 12 to 14 km vertical resolution of MLS. (ii) The 3 K uncertainty in the MLS temperatures corresponds to a factor of 2 to 3 uncertainty in  $S$  for temperatures of 140 to 150 K. (iii) The coarse vertical resolution of the MLS temperatures means that near the temperature minima at the mesopause the temperatures will be biased high (and the  $S$  biased low). Convolution of the SOFIE temperature profiles [Hervig and Gordley, 2010] with the MLS temperature kernel indicate this effect would be  $\sim 14$  K. A possible high bias of MLS temperatures is supported by comparisons with SABER which show a high bias during the polar summers as noted in section 3.

[11] The average PMC albedo increases with decreasing temperature and with increasing  $S$ , as shown in Figure 3. These albedo values show the same hemispheric asymmetry seen in Figure 2 for PMC detection probability. At a given temperature or  $S$ , the coincident PMCs are brighter in the NH than in the SH. This raises the question of whether other factors are different between the two hemispheres. The hemispheric differences in the mean PMC albedo are more ambiguous than the FO. While the PMCs are brighter in the NH for the lowest temperatures and the highest saturation ratios, for temperatures greater than  $\sim 147$  K and saturation

ratios less than  $\sim 1$ , the SH PMCs are brighter. As noted above, the altitude of the 0.006 mb surface only accounts for half of the  $\sim 1$  km greater altitude of PMCs in the SH. This means that the FO and mean albedos for the SH shown in Figures 2 and 3 should be shifted to lower temperature (and higher saturation ratios) relative to the NH. This adjustment would result in increasing the north/south differences.

## 5. Discussion

[12] Figure 1 shows that the 0.006 hPa level in the NH has lower MLS temperatures than in the SH, with an average of 146.1 K versus 149.7 K. For the PMC events the mean temperatures are 7 to 8 K cooler. The SABER climatology of Xu *et al.* [2007] shows lower temperatures in both hemispheres with a larger North/South difference [see Xu *et al.*, 2007, Figure 7]. This is qualitatively consistent with the MLS/SABER temperature differences as given by Schwartz *et al.* [2008, Figure 22] for the high latitude summer months. PMCs are detected more frequently in the NH than in the SH (11.4% vs. 5.7%). However, we note from Figures 2 and 3 that even for a given temperature or saturation ratio, there is a higher probability of detecting a PMC in the NH than the SH and there are hemispheric differences in the PMC albedo. While the brighter PMCs in the NH would be expected to increase the probability of being detected, this still does not answer the question as to why there are such differences in the brightness or FO.

[13] There are several factors which may contribute to the difference in the observed PMC/saturation relationship in the two hemispheres. One factor which may contribute to this difference is the difference in the diurnal time sampling of the MLS NH and SH measurements. The local times (LT) of the MLS measurements in the NH range from 0240–1300, while

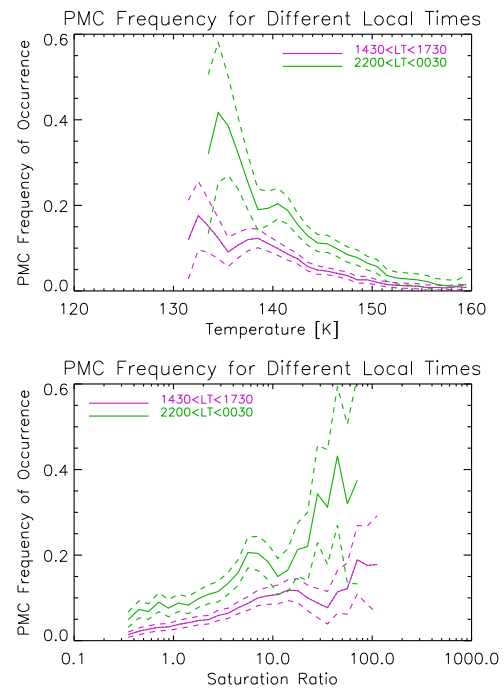


**Figure 4.** PMC frequency of occurrence in the South Hemisphere vs. temperature and saturation ratio for ascending node measurements ( $2200 < LT < 0030$ ) compared with descending node measurements ( $1420 < LT < 1730$ ).

in the SH these measurements cover completely different local times 1420–0030. Lidar measurements have shown that there are diurnal variations in the properties of PMCs [Fiedler *et al.*, 2005; Chu *et al.*, 2006], which suggests that there is a significant diurnal variation in saturation. Recent studies show that the ice particles in PMCs form and develop on time scales of hours to a few days [Rapp and Thomas, 2006; Zasetsky *et al.*, 2009], hence PMCs are likely to be sensitive not just to the saturation conditions at the time of the measurement, but to the recent history of saturation conditions.

[14] While MLS and SBUV measurements do not provide full diurnal sampling, we have compared PMC detection probabilities and albedos as a function of temperature for the ascending and descending measurements. In the SH the measurements equatorward of 80S were binned separately into  $2200 < \text{LT} < 0030$  and  $1420 < \text{LT} < 1730$  bins, while in the NH we separated  $0300 < \text{LT} < 0530$  from  $1000 < \text{LT} < 1300$ . In the NH these times are near the times of the PMC FO maximum and minimum respectively as seen by lidar [Fiedler *et al.*, 2005], which is consistent with the SBUV/2 results. In the SH the times of the SBUV/2 measurements are between the times of the extremes at Rothera [Chu *et al.*, 2006]. When looking as a function of temperature in the NH these distributions did not differ significantly except for the FO values for temperatures in the 134–138 K range (at lower temperatures there were not enough ascending node measurements for a statistically meaningful sample). In the SH the distributions for albedo as a function of temperature did not differ significantly, but the FO, as shown in Figure 4, did differ significantly. Thus, the local time of the measurements could contribute to the hemispheric differences in the dependence of the PMC FO as function of T or S but with only limited LT differences in the NH, it might not be the primary factor. There are additional differences in conditions between the NH and SH which could also contribute to the observed PMC differences.

[15] For example, hemispheric differences in the gravity wave activity and associated drag effects on the wind and temperature resulting from weaker gravity wave drag in the SH upper mesosphere [Dowdy *et al.*, 2001; Siskind *et al.*, 2003] have been suggested to be the cause of the warmer SH mesosphere. Larger temperature fluctuations in the NH could increase particle formation rates, thus contributing to greater efficiency in ice production. Chandran *et al.* [2010] have found that there are longitudinal variations in the gravity wave forcing that might also play a role.

[16] There is still some uncertainty whether the PMC ice particles initially form by heterogeneous processes on meteoric smoke particles, sulfuric acid droplets, or heavy ions in the upper mesosphere [Rapp and Thomas, 2006], or whether homogeneous nucleation is also a contributor particularly in the cold troughs of gravity wave perturbations [Murray and Jensen, 2010]. In either case hemispheric differences in the availability of these ice nuclei, or the more frequent occurrences of extremely low temperatures (favoring homogeneous nucleation) could account for the observed differences in the PMC FO.

[17] We plan to extend this analysis using PMC observations from the Ozone Monitoring Instrument (OMI), also flying on the Aura satellite. The smaller pixel size of OMI (13 km  $\times$  48 km at nadir) increases its sensitivity for PMC detection [DeLand *et al.*, 2010]. Since OMI also has coincident observations with MLS on every orbit, these data will

provide a huge increase in the number of available coincident events for our analysis. Possible other improvements would be to use IR solar occultation instruments such as SOFIE [Hervig and Gordley, 2010] or ACE [Petelina and Zasetsky, 2009] which provides better vertical resolution and can directly infer the temperature of the ice from the shape of the 3 micron absorption band.

[18] **Acknowledgments.** Most of this work was supported by grants from NASA's Science Office. Parts of E. P. Shettle's and G. E. Nedoluha's work were supported by NRL internal funding (from ONR). G. Thomas was supported under the NASA AIM satellite project.

## References

- Chandran, A., D. W. Rusch, A. W. Merkel, S. E. Palo, G. E. Thomas, M. J. Taylor, S. M. Bailey, and J. M. Russell III (2010), Polar mesospheric cloud structures observed from the cloud imaging and particle size experiment on the Aeronomy of Ice in the Mesosphere spacecraft: Atmospheric gravity waves as drivers for longitudinal variability in polar mesospheric cloud occurrence, *J. Geophys. Res.*, **115**, D13102, doi:10.1029/2009JD013185.
- Chu, X., P. J. Espy, G. J. Nott, J. C. Dietrich, and C. S. Gardner (2006), Polar mesospheric clouds observed by an iron Boltzmann lidar at Rothera (67.5°S, 68.0°W), Antarctica from 2002 to 2005: Properties and implications, *J. Geophys. Res.*, **111**, D20213, doi:10.1029/2006JD007086.
- DeLand, M. T., E. P. Shettle, G. E. Thomas, and J. J. Olivero (2003), Solar backscattered ultraviolet (SBUV) observations of polar mesospheric clouds (PMCs) over two solar cycles, *J. Geophys. Res.*, **108**(D8), 8445, doi:10.1029/2002JD002398.
- DeLand, M. T., E. P. Shettle, G. E. Thomas, and J. J. Olivero (2007), Latitude-dependent long-term variations in polar mesospheric clouds from SBUV version 3 PMC data, *J. Geophys. Res.*, **112**, D10315, doi:10.1029/2006JD007857.
- DeLand, M. T., E. P. Shettle, P. F. Levelt, and M. G. Kowalewski (2010), Polar mesospheric clouds (PMCs) observed by the ozone monitoring instrument (OMI) on Aura, *J. Geophys. Res.*, doi:10.1029/2009JD013685, in press.
- Dowdy, A., R. A. Vincent, K. Igarashi, Y. Murayama, and D. J. Murphy (2001), A comparison of mean winds and gravity wave activity in the northern and southern polar MLT, *Geophys. Res. Lett.*, **28**, 1475–1478, doi:10.1029/2000GL012576.
- Eremenko, M. N., S. V. Petelina, A. Y. Zasetsky, B. Karlsson, C. P. Rinsland, E. J. Llewellyn, and J. J. Sloan (2005), Shape and composition of PMC particles derived from satellite remote sensing measurements, *Geophys. Res. Lett.*, **32**, L16S06, doi:10.1029/2005GL023013.
- Fiedler, J., G. Baumgarten, and G. von Cossart (2005), Mean diurnal variations of noctilucent clouds during 7 years of lidar observations at ALOMAR, *Ann. Geophys.*, **23**, 1175–1181, doi:10.5194/angeo-23-1175-2005.
- Heath, D. F., A. J. Krueger, H. R. Roeder, and B. D. Henderson (1975), The solar backscatter ultraviolet and total ozone mapping spectrometer (SBUV/TOMS) for Nimbus G, *Opt. Eng.*, **14**, 323–331.
- Hervig, M., and L. L. Gordley (2010), The temperature, shape, and phase of mesospheric ice from SOFIE observations, *J. Geophys. Res.*, **115**, D15208, doi:10.1029/2010JD013918.
- Hervig, M., and D. Siskind (2006), Decadal and inter-hemispheric variability in polar mesospheric clouds, water vapor, and temperature, *J. Atmos. Sol. Terr. Phys.*, **68**, 30–41, doi:10.1016/j.jastp.2005.08.010.
- Hervig, M., R. E. Thompson, M. McHugh, L. L. Gordley, J. M. Russell III, and M. E. Summers (2001), First confirmation that ice is the primary component of polar mesospheric clouds, *Geophys. Res. Lett.*, **28**, 971–974, doi:10.1029/2000GL012104.
- Lambert, A., et al. (2007), Validation of the Aura Microwave Limb Sounder middle atmosphere water vapor and nitrous oxide measurements, *J. Geophys. Res.*, **112**, D24S36, doi:10.1029/2007JD008724.
- Lübken, F.-J., G. Baumgarten, J. Fiedler, M. Gerding, J. Höffner, and U. Berger (2008), Seasonal and latitudinal variation of noctilucent cloud altitudes, *Geophys. Res. Lett.*, **35**, L06801, doi:10.1029/2007GL032281.
- Murphy, D. M., and T. Koop (2005), Review of the vapour pressures of ice and supercooled water for atmospheric applications, *Q. J. R. Meteorol. Soc.*, **131**, 1539–1565, doi:10.1256/qj.04.94.
- Murray, B. J., and E. J. Jensen (2010), Homogeneous nucleation of amorphous solid water particles in the upper mesosphere, *J. Atmos. Sol. Terr. Phys.*, **72**, 51–61, doi:10.1016/j.jastp.2009.10.007.

- Petelina, S. V., and A. Y. Zasetsky (2009), Temperature of mesospheric ice retrieved from the O-H stretch band, *Geophys. Res. Lett.*, **36**, L15804, doi:10.1029/2009GL038488.
- Rapp, M., and G. E. Thomas (2006), Modeling the microphysics of mesospheric ice particles: assessment of current capabilities and basic sensitivities, *J. Atmos. Sol. Terr. Phys.*, **68**, 715–744, doi:10.1016/j.jastp.2005.10.015.
- Schwartz, M. J., et al. (2008), Validation of the Aura Microwave Limb Sounder temperature and geopotential height measurements, *J. Geophys. Res.*, **113**, D15S11, doi:10.1029/2007JD008783.
- Siskind, D. E., S. D. Eckermann, J. P. McCormack, M. J. Alexander, and J. T. Bacmeister (2003), Hemispheric differences in the temperature of the summertime stratosphere and mesosphere, *J. Geophys. Res.*, **108**(D2), 4051, doi:10.1029/2002JD002095.
- Thomas, G. E., R. D. McPeters, and E. J. Jensen (1991), Satellite observations of polar mesospheric clouds by the Solar Backscattered Ultraviolet radiometer: Evidence of a solar cycle dependence, *J. Geophys. Res.*, **96**, 927–939, doi:10.1029/90JD02312.
- Waters, J. W., et al. (2006), The Earth Observing System Microwave Limb Sounder (EOS MLS) on the Aura satellite, *IEEE Trans. Geosci. Remote Sens.*, **44**, 1075–1092, doi:10.1109/TGRS.2006.873771.
- Wrotny, J. E., and J. M. Russell III (2006), Interhemispheric differences in polar mesospheric clouds observed by the HALOE instrument, *J. Atmos. Sol. Terr. Phys.*, **68**, 1352–1369, doi:10.1016/j.jastp.2006.05.014.
- Xu, J., H.-L. Liu, W. Yuan, A. K. Smith, R. G. Roble, C. J. Mertens, J. M. Russell III, and M. G. Mlynczak (2007), Mesopause structure from Thermosphere, Ionosphere, Mesosphere, Energetics, and Dynamics (TIMED)/Sounding of the Atmosphere Using Broadband Emission Radiometry (SABER) observations, *J. Geophys. Res.*, **112**, D09102, doi:10.1029/2006JD007711.
- Zasetsky, A. Y., S. V. Petelina, R. Remorov, C. D. Boone, P. F. Bernath, and E. J. Llewellyn (2009), Ice particle growth in the polar summer mesosphere: Formation time and equilibrium size, *Geophys. Res. Lett.*, **36**, L15803, doi:10.1029/2009GL038727.
- 
- M. T. DeLand, Science Systems and Applications, Inc., 10210 Greenbelt Rd., Ste. 600, Lanham, MD 20706, USA.
- G. E. Nedoluha and E. P. Shettle, Naval Research Laboratory, Code 7227, 4555 Overlook Ave. SW, Washington, DC 20375, USA. (eshettle@comcast.net)
- J. J. Olivero, Department of Physical Sciences, Embry-Riddle Aeronautical University, 306 Lehman Bldg., Daytona Beach, FL 32114, USA.
- G. E. Thomas, Laboratory for Atmospheric and Space Physics, University of Colorado, 1234 Innovation Drive, Boulder, CO 80303-7814, USA.